

Superficially, result (a) seems surprising since CH₂CF₂⁻ and C₂F₄⁻ can be isolated in low temperature matrices [21], while C₂H₄⁻ has never been observed in the condensed phase. On the other hand, in the present experiments the *vertical* attachment energies are determined. As mentioned above, the anions are considered unstable with respect to out-of-plane distortion. That means the adiabatic energies of the anions may be considerably different to the vertical attachment energies.

In terms of potential energy surfaces the increasing width of the resonances can be described by an increasing slope of the anionic potential energy surface as illustrated schematically in Fig. 9. This suggests that the adiabatic relaxation energy may overcome the increase in the vertical attachment energy. In fact, recent calculations on the energies and geometries [11] of these anions support this picture, indicating that the energy of the fluoroethylene anion in its equilibrium position decreases upon fluorination.

Financial support from the Deutsche Forschungsgemeinschaft is gratefully acknowledged.

References

- [1] P. D. Burrow and K. D. Jordan, *Chem. Phys. Lett.* **36**, 594 (1975).
 [2] I. C. Walker, A. Stamatović, and S. F. Wong, *J. Chem. Phys.* **69**, 5532 (1978).
 [3] L. G. Christophorou, "The Lifetimes of Metastable Negative

- Ions", in: *Advances in Electronics and Electron Physics*, ed. E. Marton, Academic, New York 1978.
 [4] L. Sanche and G. J. Schulz, *Phys. Rev. A* **5**, 1672 (1971).
 [5] L. Sanche and G. J. Schulz, *Phys. Rev. A* **6**, 69 (1972).
 [6] E. Illenberger, H.-U. Scheunemann, and H. Baumgärtel, *Chem. Phys.* **37**, 21 (1979).
 [7] D. T. Birtwistle and A. Herzenberg, *J. Phys. B* **4**, 53 (1971).
 [8] K. Rohr, *J. Phys. B* **10**, 2215 (1977).
 [9] N. S. Chiu, P. D. Burrow, and K. D. Jordan, *Chem. Phys. Lett.* **68**, 121 (1979).
 [10] G. J. Verhaart, W. J. van der Hart, and H. H. Brongersma, *Chem. Phys.* **34**, 161 (1978).
 [11] M. N. Paddon-Row, N. G. Rondan, K. N. Houk, and K. D. Jordan, *J. Am. Chem. Soc.* **104**, 1134 (1982).
 [12] F. H. Dorman, *J. Chem. Phys.* **44**, 3856 (1966).
 [13] H.-U. Scheunemann, E. Illenberger, and H. Baumgärtel, *Ber. Bunsenges. Phys. Chem.* **84**, 580 (1980).
 [14] D. R. Stull and H. Prophet, Eds., *JANAF Thermochemical Tables NSRDS NBS 37* (1971).
 [15] G. Herzberg, *J. Mol. Spectrosc.* **33**, 147 (1970).
 [16] R. S. Berry and C. W. Reimann, *J. Chem. Phys.* **38**, 1540 (1963).
 [17] D. Feldmann, *Z. Naturforsch. A* **25**, 621 (1970).
 [18] J. L. Franklin, J. G. Dillard, H. M. Rosenstock, J. T. Herron, K. Draxl, and F. H. Field, *NSRDS NBS 26* (1969).
 [19] H. W. Jochims, W. Lohr, and H. Baumgärtel, *Nouv. J. Chim.* **3**, 109 (1979).
 [20] J. M. Simmie and E. Tschuikow-Roux, *J. Phys. Chem.* **74**, 4075 (1970).
 [21] J. T. Wang and F. Williams, *J. Am. Chem. Soc.* **103**, 2902 (1981).

(Eingegangen am 14. Oktober 1983, E 5564
 endgültige Fassung am 20. März 1984)

ArF Laser (193 nm) Photolysis of HNO₃. Formation of Excited Fragments

Th. Papenbrock, H. K. Haak, and F. Stuhl

Ruhr-Universität, Physikalische Chemie I, D-4630 Bochum, West-Germany

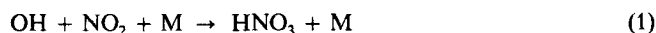
Fluorescence / Gases / Light, Emission / Multi-photon Processes / Photochemistry

HNO₃ was photolysed using an ArF (193 nm) excimer laser. Besides strong emission from OH(A²Σ⁺), weaker fluorescence from excited NO₂* was observed in the investigated wavelength range 130–900 nm. The OH(A) emission is generated by absorption of two laser photons while the NO₂* emission is produced by a one-photon process. The rotational and vibrational populations of the OH fragments can be explained by a simplified impulsive model with additional contributions from the change of the OH bond length and by a slight bending motion of the parent molecule.

Monitoring the strong OH emission appears to be a sensitive method to detect gaseous nitric acid in air in the ppb range.

Introduction

Nitric acid is an important trace constituent of the atmosphere [1]. It can be formed by reactions such as [2]



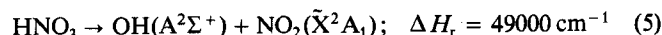
The presence of this acid is hence indicative for the HO_x and NO_x chemistry which occurs in the atmosphere.

The uv absorption spectrum of nitric acid is continuous with a relatively high absorption cross section around 200 nm ($\sigma(200 \text{ nm}) \approx 8 \cdot 10^{-18} \text{ cm}^2$) [3, 4]. The uv photolysis of HNO₃ is known to generate ground state OH and NO₂ in the wavelength range 200–315 nm [4, 5].



The quantum yield for this process has been determined to be close to one [5]. The uv photolysis of HNO₃ therefore appears to be a suitable source of hydroxyl radicals which has been used in previous excimer laser experiments [6].

Although the formation of excited OH(A²Σ⁺) is energetically possible at wavelengths below 204 nm,



no OH(A²Σ⁺ → X²Π) emission has been previously observed at photolysis wavelengths, λ, above 147.5 nm [7]. At λ > 110 nm, the quantum yield of this emission is at most 2% [7]. At the wavelength of 240 nm, the photon energy is sufficient to generate excited NO₂(²B₂) up to the dissociation limit of ground state NO₂



In Reaction (6) the enthalpy of reaction was calculated for possible NO₂* emission at 600 nm. However, NO₂* fluorescence has

not been detected previously and the quantum yield of this emission has been therefore estimated to be less than 0.5% at the photolysis wavelength of 123.6 nm [7].

During studies of emissions generated by ArF (193.34 nm Δ 51722 cm⁻¹) excimer laser photolysis of small molecules [8] we unexpectedly observed OH(A² Σ^+ \rightarrow X² Π) emission when photolysing NO₂ [9]. Since HNO₃ was stated by the manufacturer to be a probable impurity of our sample we subsequently photolysed HNO₃ in separate experiments. As a result, we observed very strong OH emission which easily could be rotationally resolved. Moreover, excited NO₂^{*} molecules were observed [9].

Besides those processes which generate excited OH^{*} and NO₂^{*} in the ArF laser photolysis of HNO₃, we would like to discuss briefly the feasibility of detecting HNO₃ molecules in air by generating excited photodissociation fragments.

Experimental

The apparatus used for the present spectroscopic investigation has been described previously in detail [8]. Briefly, an unfocused ArF excimer laser beam (193.3 nm; 10 to 150 mJ cm⁻²) was used to irradiate flowing samples of HNO₃ and added gas. Fluorescence emissions were observed during or after the laser pulse using short aperture durations of 0.5–1 μ s of a boxcar integrator. Fluorescence was investigated in the wavelength range 130–900 nm using a 0.5 m-monochromator (Minuteman).

In some experiments, the monochromator was replaced by an arrangement of optical filters, baffles and lenses. This way, the integrated OH emission at about 309 nm could be measured with high sensitivity. In order to minimize saturation of the photomultiplier (EMI 9789 QB) by the intense fluorescence obtained at high concentrations of HNO₃, two filters (maximum transmission of 20% and 52% at 309.0 and 308.8 nm, FWHM 7.0 and 4.1 nm, respectively) were used together and the focusing lenses were omitted. Unfortunately, the sensitivity of this detection method was hampered by a strong light pulse of about 40 ns width and a weaker pulse of several hundred ns width which always were observed even with the fluorescence cell evacuated. The short pulse might be due to stray light from the discharge of the laser system; the slower decay is probably caused by fluorescence of the suprasil windows of the cell. Further work is planned to reduce these interfering signals.

With this arrangement, the gate position of the boxcar integrator was therefore delayed not to open till 20 ns after the laser shot. In order to obtain sufficiently low concentrations of HNO₃ in dry air a flowing mixing system was used. A part of the flow was bubbled through liquid HNO₃ the temperature of which was kept constant below room temperature. This flow was further diluted twice in order to obtain mixing ratios which were calculated to be in the ppb range and larger. This mixing system consisted mainly of glass and partly of stainless steel (needle valves). We are therefore aware that some of the HNO₃ molecules will be lost due to the metal walls in this system [10].

The HNO₃ sample used had a stated (Riedel de Haen) purity of >99.5%. For some spectroscopic experiments, HNO₃ was distilled. The HNO₃ sample was always stored in the dark. The minimum (stated) purities of the other gases used were: synthetic air, 99.9%; Ar, 99.997%; N₂, 99.99% (Messer, Griesheim).

Results

Upon irradiation of nitric acid with light from the ArF laser, several emissions were observed in the wavelength range from 150 to 900 nm. At wavelengths below 280 nm, fluorescence from excited NO molecules was observed. Since the intensity distribution of this emission was similar to that found in the ArF laser photolysis of NO₂ [9] we infer that a significant amount of NO₂ is present in this photolysis system as an impurity.

At $\lambda > 280$ nm, very strong emissions from OH(A² Σ^+) and weaker emission from electronically excited NO₂^{*} were observed as shown in

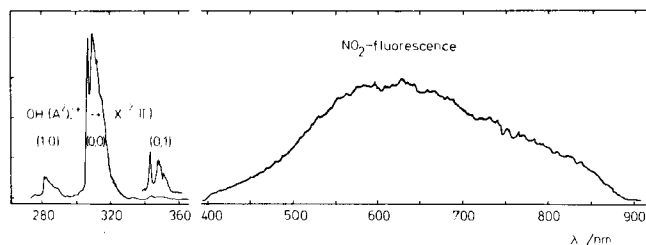


Fig. 1

Spectrum of the fluorescence in the wavelength range 270 to 900 nm. The spectral resolution is 0.85 nm. The laser energy was 45 mJ cm⁻² and the aperture duration 500 ns. The sensitivity scales and the pressures of HNO₃ are different for the two wavelength intervals shown: 270 to 360 nm (0.04 mbar HNO₃) and 400 to 900 nm (0.1 mbar HNO₃)

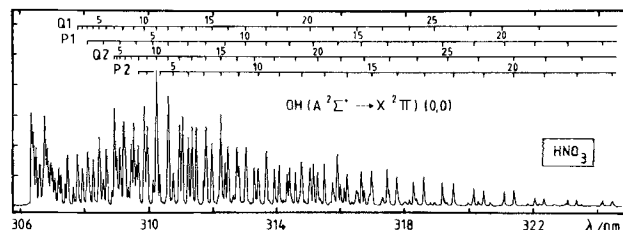


Fig. 2

Rotationally resolved emission spectrum of OH(A² Σ^+ , $v' = 0 \rightarrow$ X² Π , $v'' = 0$). The spectral resolution is 0.05 nm. The pressure of HNO₃ was 0.04 mbar. The laser was used at 70 mJ cm⁻²; the aperture duration was 500 ns

Fig. 1. It should be noted in Fig. 1 that the experimental conditions for each of the emissions were different.

The rotationally resolved OH(A² Σ^+ , $v' = 0 \rightarrow$ X² Π , $v'' = 0$) band is shown in Fig. 2. Rotationally excited levels up to $N' = 31$ can be detected. This spectrum obviously indicates a high rotational temperature. This temperature was determined using the emission from $N' = 10$ to 23 to be 8500 ± 500 K at 0.04 mbar HNO₃ and 70 mJ cm⁻². For lower and higher values of N' , the emissions were slightly lower than predicted by this temperature. At high values of N' , this is most likely due to the onset of predissociation at $N' > 23$ [11]. The rotational temperature was observed to be independent of pressure of HNO₃ in the range 0.06 to 0.26 mbar and found to decrease somewhat ($\sim 30\%$) upon the addition of air (2.8 mbar). This decrease in temperature is most likely due to partial relaxation by N₂ before electronic quenching becomes effective [12]. Furthermore, some enhancement (from ~ 7000 to 10000 K) of the rotational temperature was observed with increasing laser intensity (10 to 140 mJ/cm²).

From the intensities of the rotational lines such as those displayed in Fig. 2, the relative population, N_{rel} , was calculated for the rotational quanta N' in the excited OH(A² Σ^+ , $v' = 0$)-state. The result is shown in Fig. 3 for the emissions of the P₁, P₂, Q₁ and Q₂ branches. Included in this figure is the nascent rotational distribution of ground state OH(X² Π , $v'' = 0$) obtained by Jacobs et al. [13] in the ArF laser photolysis of 0.027 mbar HNO₃.

Lifetime measurements of the OH emission at $\lambda = 309 \pm 1$ nm were performed as a function of pressure of HNO₃. The fluorescence lifetime extrapolated to zero pressure was measured to be $\tau_{\text{F}}^0 = 690 \pm 60$ ns and the effective quenching rate constant $k_{\text{Q}}(\text{HNO}_3)$ was determined to be $(5.1 \pm 2) \cdot 10^{-10}$ cm³ s⁻¹ at the present experimental conditions (~ 35 mJ/cm²). The error limits represent three times the standard deviation. It should be noted that this value of $k_{\text{Q}}(\text{HNO}_3)$ might include small contributions by the photolysis products.

The fluorescence intensity (at 308.8 nm, spectral resolution 0.03 nm) was also measured as a function of pressure of HNO₃ (0.033 to 0.59 mbar). A usual fluorescence curve was obtained exhibiting linear increase in intensity at low pressures and a maximum intensity at about 0.08 mbar.

The dependence of the fluorescence intensity on the laser intensity is shown in Fig. 4 in a double logarithmic plot. The slope obtained for the

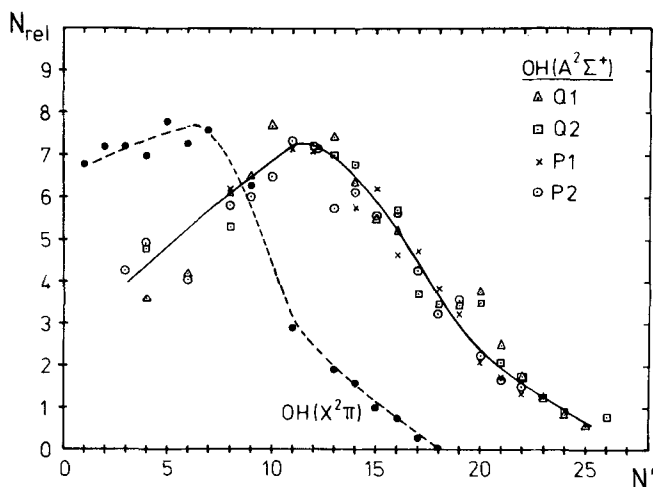


Fig. 3
Relative population of $\text{OH}(A^2\Sigma^+, v' = 0)$ as a function of rotational level N' , (open symbols). The data is obtained from the spectrum of Fig. 2 for the \times , P_1 ; \circ , P_2 ; \triangle , Q_1 ; and \square , Q_2 branches. Included is the population recently reported [13] for the generation of ground state $\text{OH}(X^2\Pi, v'' = 0, N'')$ (full circles)

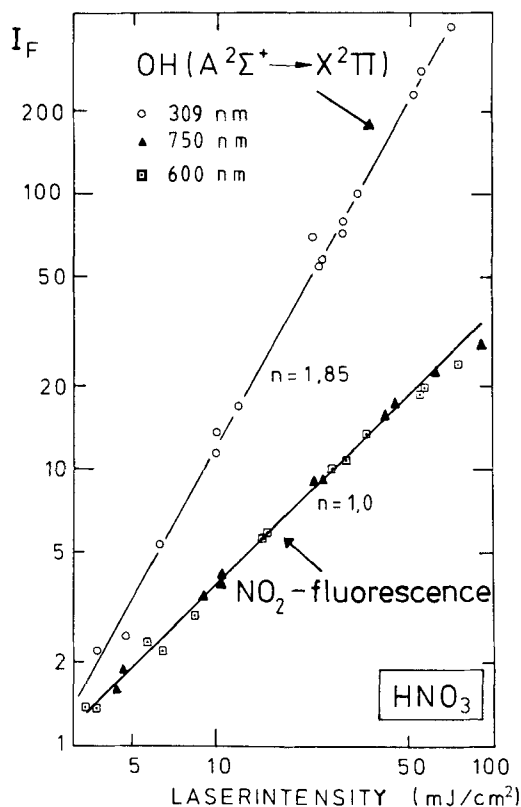


Fig. 4
Double logarithmic plot of the fluorescence intensity, I_F , vs. the laser intensity. The data for OH emission is shown by open circles (\circ). It was taken at 308.8 ± 0.025 nm in the photolysis of 0.26 mbar HNO_3 using an aperture duration of 500 ns. The data for NO_2 emission is shown by triangles and squares. It was taken at both 600 (\square) and 750 nm (\blacktriangle) in the photolysis of 0.053 mbar HNO_3 using an aperture duration of 270 ns

straight line is $n = 1.85$. Also included in this figure is the corresponding data for the NO_2^* emission.

In order to test how sensitive the detection of HNO_3 by excited OH is, we have mixed small amounts of HNO_3 in flowing air. The emission

was monitored at 308.8 nm using a slit width of 150 μm (spectral resolution of 0.25 nm). This way, a detection limit of 10 ppm HNO_3 was obtained. Using the Stern-Volmer-mechanism, the quenching rate constant for the addition of air was determined to be $2.5 \cdot 10^{-11} \text{ cm}^3 \text{ s}^{-1}$.

In the observed wavelength region, this value might be influenced by processes such as relaxation and hence represents an effective quenching constant. To further increase the sensitivity of the OH fluorescence detection, the monochromator was replaced by the arrangement of interference filters. The measurements were performed as described in the experimental section.

Using the interference filters, the OH fluorescence intensity was found to be very intense. Peak currents above 1 mA at the anode of the photomultiplier were easily obtained for mixing ratios greater than 200 ppb HNO_3 . A calibration of the fluorescence signal was attempted for mixing ratios ranging from 20 to 1000 ppb. The calibration curves representing fluorescence signal vs. mixing ratio were found to be non-linear. The detection limit was estimated for the present preliminary set up to be about 4 ppb. No interfering emission was observed for H_2O , H_2O_2 , CH_3OH and $\text{C}_2\text{H}_5\text{OH}$.

Some properties of the NO_2^* emission were investigated briefly in this study to confirm the proposed identification. The lifetime was found to be longer than 13 μs , the lower limit being determined by diffusion. The quenching constants by the parent molecule HNO_3 and by N_2 were measured to be $(1.6 \pm 0.3) \cdot 10^{-10}$ and $(4 \pm 1) \cdot 10^{-11} \text{ cm}^3 \text{ s}^{-1}$ at the present experimental conditions. The error limits represent three times the standard deviation. The dependence of the NO_2^* fluorescence intensity on the laser intensity is shown in Fig. 4. At both wavelengths 600 and 750 nm, a linear dependence was measured (slope $n = 1.0$).

Discussion

It is known that the uv photolysis of HNO_3 generates NO_2 and OH in their ground states with a quantum yield of about one [4, 5] (Reaction (4)). At 193.3 nm, only $\sim 3\%$ of the photodissociation excess energy shows up as rotation of $\text{OH}(X^2\Pi)$; no vibrational excitation has been observed [13]. The absorption cross section for this wavelength is about $1.1 \cdot 10^{-17} \text{ cm}^2$ [3]. With this cross section, about 70% of the parent molecules are destroyed during a laser shot of 120 mJ cm^{-2} . Hence, the ArF laser photolysis presents a very efficient method to generate ground state OH radicals and, obviously, several tenths mbar of $\text{OH}(X^2\Pi)$ can be easily formed in the unfocused laser beam. Besides OH , large amounts of NO_2 are formed. It is therefore not surprising to detect additional photolysis products such as excited NO which have been previously observed in the ArF laser photolysis of NO_2 [9].

The energy of one ArF laser photon is sufficient to generate excited OH in the $(A^2\Sigma^+, v' = 0)$ -state (Reaction (5)) up to rotational quanta $N' \leq 12$. The excess energy ($\sim 2600 \text{ cm}^{-1}$) does not suffice to excite the first vibrational level of the $(A^2\Sigma^+)$ -state (2989 cm^{-1}). The spectra in Figs. 1 and 2 however demonstrate that both $v' = 1$ and $N' > 12$ become populated in the present experiments. We therefore conclude that these emissions must be generated by absorption of several (most likely two) photons. This conclusion is confirmed by the results displayed in Fig. 4, which indicate that the observed OH emission is due to absorption of (at least) two laser photons. It is also consistent with the result obtained by Okabe [7] who observed the one-photon generation to occur in the vuv photolysis of HNO_3 at wavelengths below 148 nm.

The probability to form excited OH via absorption of a second laser photon by a nascent photodissociation fragment is thought to be small for the following reason. The only products known to be formed are ground state OH and NO_2 [2, 3]. The production of other radicals at 193 nm containing OH such as

HOX with X=N, NO, O or O₂ appears to be unlikely. The OH(X²Π) radicals are known to be formed with very little excess energy [13] and can not be excited by a second laser photon to yield the observed emission.

We therefore believe that two-photon excitation takes place sequentially in the parent molecule. In spite of the unstructured uv-spectrum [3, 4] which indicates direct photo-dissociation by the first absorbed photon, the absorption of the second ArF laser photon appears to be rather efficient. Namely, this OH fluorescence is the most intense emission so far observed in our studies of a number of chlorinated compounds such as COCl₂, CCl₄ [14], ammonia and related species [8], and NO₂ [9].

The population distribution in the rotational and vibrational states may be indicative for the dynamics of the photo-fragmentation. The excess energy, $E_{\text{avl}} = 54241 \text{ cm}^{-1}$, which is available beyond the energy required to form fragments is distributed among the rotational, vibrational and translational energies of the products, E_{rot} , E_{vib} and E_{trans} , respectively. For the vibrationally population ratio $N(v' = 1)/N(v' = 0)$, a value of 0.34 is calculated using the integrated intensities of the (1,0) and (0,0) bands of Fig. 1, the calibrated spectral sensitivity of the detection system and known Einstein transition probabilities [15]. From this ratio and from the rotational temperature, the fractions of the excess energy being converted to rotation and vibration of OH(A²Σ⁺) are calculated to be $E_{\text{vib}}/E_{\text{avl}} = 0.014$ and $E_{\text{rot}}/E_{\text{avl}} = 0.108$. These values and those obtained by other authors [7, 13] are listed in Table 1 together with values estimated by using a simple impulsive model. In our estimate for E_{rot} , the value was taken to be kT ; for E_{vib} , predissociation in the $v' = 0$ state for $N' > 23$ and in the $v' = 1$ state for $N' > 14$ was not taken into account.

Table 1
Energy partitioning of the available excess energy into the rotational and vibrational degrees of freedom of the OH fragment

	Experimental			Impulsive model (calculation for $\chi = 103^\circ$)	
	OH(A ² Σ ⁺)		OH(X ² Π)	(calculation for $\chi = 103^\circ$)	
	This work	Ref. [7]	Ref. [13]	A = NO ₂	A = N
$E_{\text{vib}}/E_{\text{avl}}$	0.014	0.02	<0.004	0.0022	0.0014
$E_{\text{rot}}/E_{\text{avl}}$	0.108	0.07	0.03	0.042	0.026

In a different photolysis experiment using the irradiation of HNO₃ by the Kr line at 123.6 nm, Okabe [7] has previously determined the fractional energies which show up as vibrational and rotational excitation of OH(A²Σ⁺). His results demonstrate (Table 1) that the conversion of excess energy is similarly effective in both his and the present experiment. On the other hand, Jacobs et al. [13] have recently determined the energy partitioning in the one-photon-dissociation of HNO₃ by an ArF excimer laser leading to NO₂ and OH in their ground states. As demonstrated by the data displayed in Table 1, their result is different from those obtained in the present and in Okabe's [7] work. Particularly, the lack of detectable vibrational excitation [13] is in contrast to the present observation.

We have therefore estimated the energy expected for the rotational and vibrational excitation of a diatomic molecule BC according to a simple impulsive model [16]. In this model, the triatomic molecule ABC photodissociates directly to break the

bond A-BC on a repulsive potential surface. Previously, similar estimates have successfully explained the direct photodissociation of several small molecules [7, 13, 16–18].

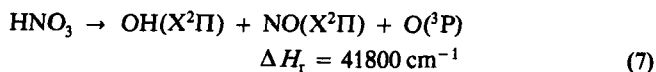
The calculations were performed for an ABC bond angle $\chi = 103^\circ$ at the time of the dissociation which corresponds to the value of the H–O–N bond in HNO₃ in the ground state [19]. To represent the mass A in this model, we used either that of NO₂ or N assuming either infinitely stiff or infinitely soft NO₂ bonds. The corresponding two sets of data for $E_{\text{vib}}/E_{\text{avl}}$ and $E_{\text{rot}}/E_{\text{avl}}$ are displayed in Table 1. Realistic values from this classical quasidiatomic model lie between the data of both sets depending on the stiffness of the NO₂ bonds. A comparison of the calculated data in Table 1 with the experimental values reveals that the calculation supports the results by Jacobs et al. [13] rather than those obtained by Okabe [7] and by the present work.

This discrepancy is most severe for vibrational excitation (order of magnitude difference) while, for rotational excitation, an enhancement of only a factor of ≈ 2 to 3 is observed in Okabe's [7] and the present experiments. This additional rotational excitation has been explained by Okabe [7] by a small change ($\approx 3^\circ$) of the bond angle H–O–N during the photon absorption process. The resulting small bending vibration is sufficient to excite the observed rotation of the diatomic fragments [7]. The additional vibrational excitation which is observed in the experiments with high photon energies leading to excited OH(A²Σ⁺) might be due to a change in bond length of the fragment OH. The length of this bond in the ground state of HNO₃ is 0.096 nm [19]. It increases when forming excited OH(A²Σ⁺) to become 0.101 nm [11] but does not alter for the generation of ground state OH(X²Π) (0.097 nm [11]). It is therefore likely that this increase in bond length leaves a fraction ($\approx 25\%$) of the departing OH(A²Σ⁺) molecules vibrationally excited.

In summary, the photofragmentation of HNO₃ yielding OH occurs directly without great structural change in the parent molecule. Deviations from the simple impulsive model can be explained by a slight bending motion of the highly excited parent molecule and by a change in bond length when electronically excited OH are formed. The OH radicals are expected to have large translational energies. Unfortunately, the spectral resolution is so small that the resulting Doppler broadening of the lines cannot be observed.

Formation of excited NO₂^{*} has not been observed previously in the photolysis of HNO₃ [7]. The observed fluorescence appears continuous at the spectral resolution used and it cannot be decided from the spectrum which of the excited states (²B₂ or ²B₁) is responsible for the emission. The data of Fig. 4 indicates that the NO₂^{*} emission is caused by the absorption of one photon. The intensity of this emission is weak compared with that observed from the OH(A²Σ⁺) state which is generated in a two photon process. We hence conclude that this process producing NO₂^{*} is a minor photodissociation channel. This conclusion is in accord with the fact that NO₂^{*} has not been observed in the previous photolysis experiments by Okabe [7].

It should be noted in Fig. 1 that the NO₂^{*} emission extends to wavelengths down to 398 nm which corresponds to the dissociation limit of NO₂ [4]. We therefore believe that, additionally, the photodissociation process



occurs. Then, an excess energy of about 10000 cm^{-1} is available for distribution among the three products. Whether this process excites vibration and/or rotation in $\text{NO}(\text{X}^2\Pi)$ is not known. The production of $\text{O}(\text{D})$ in Reaction (7) is energetically not possible.

Lifetime measurements which were routinely performed in our ArF laser studies confirm the proposed identifications. Particularly, the value of the fluorescence lifetime of $\text{OH}(\text{A}^2\Sigma^+)$ is in excellent agreement with literature values [11]. This agreement indicates that no radiation trapping occurs in this system in spite of the large amounts of ground $\text{OH}(\text{X}^2\Pi)$ formed. If trapping occurred it probably would distort the measurement of the rotational distribution. The absence of detectable trapping is in agreement with the experience we have gained with absorption measurements of OH at similar optical densities [20]. The values for the effective rate constants of the quenching of $\text{OH}(\text{A}^2\Sigma^+)$ and NO_2^* by the parent molecule are influenced by the large amounts of photolysis products present after the laser shot. They are therefore not considered to be accurate numbers but very crude estimates. The present rate constant for the quenching of the $\text{OH}(\text{A}^2\Sigma^+)$ emission by air most likely represents a lower limit since relaxing $\text{OH}(\text{A}^2\Sigma^+)$ with large values of N' can contribute to the present lifetime measurements at $\lambda = 309 \text{ nm}$. The value of the rate constant for the quenching of NO_2^* by N_2 is in agreement with literature values [21].

The detection of HNO_3 by $\text{OH}(\text{A}^2\Sigma^+)$ emission in the ArF laser photolysis appears to be very sensitive. The preliminary experiments performed here still suffer from several shortcomings: (a) a strongly interfering signal at 308 nm when using the interference filter, (b) nonlinearity of the calibration curve which might be due to photomultiplier signals which were too large, (c) calibration of concentrations with an inappropriate mixing system and (d) an incomplete study of possible interfering gases. Since the present detection limit in the ppb-range is very promising we intend to investigate further the feasibility of detecting low concentrations of HNO_3 in air by this method.

We gratefully acknowledge financial support by the Deutsche Forschungsgemeinschaft (SFB 42) and Land NRW. Some equipment was provided by UBA project 10.402.421.

References

- [1] P. A. Leighton, "Photochemistry of Air Pollution", Academy, New York 1961.
- [2] J. G. Calvert and W. R. Stockwell, *Environ. Sci. Technol.* **17**, 429A (1983).
- [3] F. Biau, *J. Photochem.* **2**, 139 (1973/74); H. S. Johnston and R. Graham, *J. Phys. Chem.* **77**, 62 (1973).
- [4] H. Okabe, "Photochemistry of Small Molecules", Wiley, New York 1978.
- [5] H. S. Johnston, S. G. Chang, and G. Whitten, *J. Phys. Chem.* **78**, 1 (1974).
- [6] H. H. Nelson, W. J. Marinelli, and H. S. Johnston, *Chem. Phys. Lett.* **78**, 495 (1981); B. Fritz, K. Lorenz, W. Steinert, and R. Zellner, in: "Physico-Chemical Behaviour of Atmospheric Pollutants", eds. B. Versino and H. Ott, Reidel, Dordrecht 1982; A. R. Ravishankara, F. L. Eisele, and P. H. Wine, *J. Phys. Chem.* **86**, 1854 (1982).
- [7] H. Okabe, *J. Photochem.* **9**, 150 (1978); *J. Chem. Phys.* **72**, 6642 (1980).
- [8] H. K. Haak and F. Stuhl, *J. Phys. Chem.* (to be published) and references therein.
- [9] H. K. Haak and F. Stuhl, *J. Photochem.* **17**, 69 (1981).
- [10] H. I. Schiff, D. R. Hastie, G. I. Mackay, T. Iguchi, and B. A. Ridley, *Environ. Sci. Technol.* **17**, 352A (1983).
- [11] K. P. Huber and G. Herzberg, "Molecular Spectra and Molecular Structure. IV. Constants of Diatomic Molecules", Van Nostrand, New York 1979.
- [12] K. Schofield, *J. Phys. Chem. Ref. Data* **8**, 723 (1979).
- [13] A. Jacobs, K. Kleinermanns, H. Kuge, and J. Wolfrum, *J. Chem. Phys.* **79**, 3162 (1983).
- [14] H. K. Haak and F. Stuhl, *Chem. Phys. Lett.* **68**, 399 (1979); 14th Informal Conference on Photochemistry, Newport Beach, Cal., Abstract L5 (1980).
- [15] D. R. Crosley and R. K. Lengel, *J. Quant. Spectrosc. Radiat. Transfer* **15**, 579 (1975).
- [16] G. E. Busch and K. R. Wilson, *J. Chem. Phys.* **56**, 3626 (1972).
- [17] A. F. Tuck, *J. Chem. Soc. Faraday Trans. II* **689** (1977).
- [18] R. Vasudev, R. N. Zare, and R. N. Dixon, *Chem. Phys. Lett.* **96**, 399 (1983).
- [19] A. P. Cox and J. M. Riveros, *J. Chem. Phys.* **42**, 3106 (1965).
- [20] A. Hofzumahaus and F. Stuhl, *Ber. Bunsenges. Phys. Chem.* (to be published).
- [21] G. H. Myers, D. M. Silver, and F. Kaufman, *J. Chem. Phys.* **44**, 718 (1966); V. M. Donnelly, D. G. Keil, and F. Kaufman, *J. Chem. Phys.* **71**, 659 (1979).

(Eingegangen am 4. Januar 1984, E 5645
endgültige Fassung am 20. März 1984)

Optisches Verfahren zur Bestimmung der Geschwindigkeit einzelner suspendierter kolloider Teilchen

D. Busch*), G. Haase und F. Zörgiebel

Institut für Wissenschaftliche Photographie der Technischen Universität München, D-8046 Garching, Federal Republic of Germany

Colloides / Light, Scattering / Methods and Systems / Microscopic Electrophoresis / Transport Properties

Using components of a standard electrophoresis equipment (Zytopherometer) a stroboscopic dark field method was developed to record colloidal particles moving in an electric field. An argon ion laser served as a strong illuminant, a TTL electronic equipment provided the synchronization of electric field pulses, illumination and camera shutter. With this method speeds of particles – e.g. soot dispersed in cyclohexan – could be measured at field strengths from zero (Brownian movement) up to $3 \cdot 10^5 \text{ V/m}$ (beginning of turbulence)

*) Neue Adresse: Drägerwerke AG, D-2400 Lübeck.